The Amplitude Dependence of High-Frequency Spectral Decay: Constraint on Soil Non-Linearity

by Jennie A. Durward, David M. Boore, William B. Joyner

Publication information:

Durward, J. A., D . M. Boore, and W. B. Joyner (1996). The amplitude dependence of high-frequency spectral decay: Constraint on soil non-linearity, *Proceedings of International Workshop on Site Response 2*, Yokosuka, Japan, January 16--17, 1996, 82--103.

THE AMPLITUDE DEPENDENCE OF HIGH-FREQUENCY SPECTRAL DECAY: CONSTRAINT ON SOIL NON-LINEARITY

Jennie A. DURWARD[1], David M. BOORE[2], and William B. JOYNER[2]

[1]Research Assistant, U.S. Geological Survey, Menlo Park, CA 94025, USA (now at Dept. of Engineering, University of California, San Diego, California)
[2]Geophysicist, U.S. Geological Survey, Menlo Park, CA 94025, USA

SUMMARY

The high-frequency spectral-decay parameter κ measured at 23 sites from 24 earthquakes in the Imperial Valley of California increases with the peak velocity at the ground surface. This can only be due to nonlinear response of the soil, since purely linear response would show no increase. Modeling of κ using equivalent-linear calculations produces too great an increase with peak velocity, whereas simulations using nonlinear simulations show virtually no dependence of κ on peak velocity, at least with the particular constitutive relations used in the simulations. Ratios of peak acceleration to peak velocity vs. peak velocity provide another means to assess the extent of nonlinearity. Plots for the 1979 Imperial Valley mainshock show a decrease of the ratio with peak velocity, opposite to the trend expected for linear soil response, again providing evidence for nonlinear soil response. The equivalent-linear calculations agree with the observed trend, as does the nonlinear calculation with a strength coefficient (ratio of dynamic strength to vertical effective stress) of 1.0 (but not 0.33).

INTRODUCTION

Nonlinear soil response is an important issue for earthquake engineering. Calculations of nonlinear soil response are made by equivalent-linear methods (Idriss and Seed, 1968; Schnabel *et al.*, 1972) and nonlinear methods (e.g. Joyner and Chen, 1975; Pyke, 1979; Lee and Finn, 1982), using dynamic soil properties measured in the laboratory. There are grounds, however, for doubts concerning whether the laboratory data are representative of the soil *in situ* (EPRI, 1993, Appendix 7A). It is desirable therefore to confirm the calculations by real ground-motion measurements. Ideally one would use downhole data recorded at the bedrock interface and the surface. Lacking that, surface rock and nearby surface soil recordings would be desirable. Such data are few, however, particularly at the levels of motion large enough to guarantee significant nonlinearity. In this paper we take a different approach and examine strong-motion records from the Imperial Valley, California, where recordings of multiple earthquakes are available at many stations, permitting us to examine the effect of amplitude level on station response. We look at the Anderson and Hough (1984) parameter κ, which measures the decay of acceleration spectra at high frequencies, and the ratio of peak

horizontal acceleration to peak horizontal velocity. What follows is a preliminary report on our results.

DATA ANALYSIS

Anderson and Hough (1984) first introduced κ as a seismological parameter. They noted that often Fourier acceleration spectra decay almost linearly when the log of the spectrum is plotted against frequency, although in the absence of attenuation the standard ω-squared source model has a flat acceleration spectrum for frequencies sufficiently greater than the corner frequency. There has been some controversy as to whether κ depends on the source or on attenuation as the waves travel from the source to the receiver (with most of the attenuation thought to occur close to the Earth's surface). Our preference is that κ is primarily a function of attenuation in the near-surface sediments, and that is the assumption that we make here. The basic measurement of κ is made by fitting the following functional form to the Fourier spectrum of ground acceleration (S):

$$\ln S = C - \pi \kappa f.$$

We used uncorrected data from the CD-ROM of Seekins *et al.* (1992) for a set of earthquakes and stations in the Imperial Valley (Tables 1 and 2; Figure 1). We applied instrument corrections and low-cut filter corrections to the data before analysis. The low-cut filter frequencies were determined by applying a series of filters to the records and observing the plots of ground velocity, using our judgment as to the appropriate cutoff frequency; the measured values of κ are insensitive to the cutoff frequencies. We used time-domain windows with slight tapers at the ends; extensive tests showed the results not to depend on the particular windows chosen. The spectra were not smoothed. The horizontal components were combined into one spectrum by finding the square-root of the arithmetic average of the squared spectral amplitudes of each component. This combined spectrum was plotted, and a straightline was fit between $\ln S$ and f. The lower frequency of the least-squares fit was 2 Hz for events with magnitude larger than 4.1 and 5 Hz for smaller events (to be beyond the corner frequency of the event). The upper frequency was 25 Hz, a conservative value based on plots of the noise spectrum and the shape of the spectrum of the data; in a number of cases we could have used a higher frequency with little difference in the results. Sample spectra and the straight-line fit are shown in Figure 2.

Our thesis is that κ will depend on the strain amplitude if the soil response is nonlinear. To see this from our data, we decided to use peak velocity at the ground's surface as a surrogate for peak strain, and plot κ vs. peak velocity. There are other correlations in the data, however, that must be removed to isolate any dependence on strain amplitude. To remove these other correlations, we performed a multi-variable regression analysis, with the following explanatory variables: a site term for each site, a linear term in distance, and a term to differentiate between mainshock recordings (with its long extended rupture) and recordings of the other events. We used closest horizontal distance to the rupture surface as the distance measure. After several trials with various functions, we modeled the peak-velocity dependence as a cubic in log peak

velocity. The regression coefficients are given in Table 3. Using these coefficients, we corrected the observed values of κ for the site, distance, and size-of-fault coefficients. These reduced observations are plotted in Figure 3. The average κ at a velocity of 1 cm/s is 0.31. It is clear that there is a dependence of κ on peak velocity. If the soil response were purely linear, then κ would not depend on peak velocity. Clearly, that is not the case here, and therefore we have strong evidence for the nonlinear response of the soil. In the next section we test several models of nonlinear response against these and other data.

THE DEPENDENCE OF κ ON PEAK VELOCITY FOR EQUIVALENT-LINEAR AND NONLINEAR MODELS

We model the effect on κ of the soil column shown in Figure 4 using equivalent-linear and nonlinear methods. The time series for the incident wave were generated by the methods of Boore (1996) assuming a stochastic omega-squared source model (Hanks and McGuire, 1981). Amplification factors were applied so that the motions are appropriate for the shear-wave velocity at 244 m. The κ for the input motion was chosen so that the κ for the modeled surface motion would agree with the solid line in Figure 3 at a PGV of 1 cm/s. Twenty different realizations of the input motion were generated. One sample is illustrated in Figure 5. All 20 realizations were scaled to specified peak velocities and used as input to SHAKE91 (Idriss and Sun, 1992). Figure 6 shows the surface motion for the input in Figure 5 scaled to a PGV of 80 cm/s for the case where the modulus and damping of the uppermost 90 m was permitted to vary with strain. A series of values for input PGV from 1 to 100 was used. For each value of the input PGV the spectra of the surface motions were averaged over the 20 realizations and the κ was determined from the average spectrum by least-squares fitting. The results are shown in Figure 7. The long dashes correspond to the case where the modulus and damping of the whole 244 m section was permitted to vary with strain. The low-strain moduli were computed from the shear-wave velocity values in Figure 4 and assumed density values. The curve of modulus vs. strain was that given by Sun *et al* (1988), and the curve of damping vs. strain was that given by Idriss (1990). These curves were chosen as appropriate for clays. The actual materials are interbedded silty clays and clayey silts. The resulting increase in κ values with increasing PGV is greater than shown by the data. These modulus and damping curves, however, were probably never intended to be used at depths as great as 244 m. Since the ratio of strength to modulus increases with depth, the curves would be expected to change with depth (Hardin and Drnevich, 1972). For this reason, we repeated the calculations, forcing modulus and damping to be constant with strain for the materials between 90 and 244 m. The results are shown in Figure 7 by the short dashes, which agree with the data below about 10 cm/s. The results may suggest that the equivalent-linear solution may underestimate short-period surface motion at high amplitude levels, which is the conclusion reached by Joyner and Chen (1975).

For nonlinear modeling we used the program TESS (Pyke, 1979). As above, low-strain shear-wave velocities were taken from Figure 4. Below 10 m depth the soil was assumed to be normally consolidated and the dynamic strength, τ_{max} was taken as

$$\tau_{max} = C_s P_{ve}$$

where C_s is the strength coefficient and P_{ve} is the vertical effective stress. Above 10 m the preconsolidation vertical stress was assumed to be equal to the vertical effective stress at 10 m, and τ_{max} was taken as

$$\tau_{max} = C_s P_{ve} (OCR)^T$$

where OCR is the overconsolidation ratio in terms of vertical effective stress and T was given a value of 0.75 (Ladd and Edgers, 1972). No degradation was assumed and no pore-water diffusion. A sample time series at the surface is shown in Figure 8; note the relatively greater frequency content compared to the sample surface motion from SHAKE91 (Figure 6). The κ results are shown in Figure 9. The long dashes show the result for $C_s = 0.33$ (Joyner and Chen, 1975), and the short dashed show the results for $C_s = 1.0$. In terms of κ the TESS model looks like a linear system, and C_s has virtually no effect on κ. We have obtained essentially identical results (not shown here) using the nonlinear model of Joyner and Chen (1975). We suspect that the independence of κ on PGV and C_s is inherent in the hyperbolic stress-strain relationship assumed both in TESS and in the Joyner-Chen model. We are exploring modifications of the stress-strain relationship which might make the models give results more like our data.

MODELING THE ACCELERATION–VELOCITY RATIO

Since κ does not discriminate between the very different models represented by $C_s = 0.33$ and $C_s = 1.0$, we looked for another parameter to represent the ground motion and tried the ratio of peak horizontal acceleration to peak horizontal velocity. Since that ratio is strongly dependent on earthquake magnitude, we restricted our attention to the 1979 Imperial Valley mainshock. Figure 10 shows the data along with the two curves from the SHAKE91 runs, both of which fit quite well. Figure 10 also includes a curve generated by stochastic simulation, which shows the effect that distance would be expected to have if the soil were linear. Figure 11 shows the comparison for the TESS runs. The curve for $C_s = 1.0$ fits the data well, but the curve for $C_s = 0.33$ clearly does not.

Since the equivalent-linear model is really an approximate method of computation and not a physical model, we tentatively adopt the nonlinear model with $C_s = 1.0$ as our preferred model. Using that model we compute the curve of amplification vs. input acceleration shown by the solid line in Figure 12 and the curve of surface acceleration vs. input acceleration shown by the solid line in Figure 13. On Figures 12 and 13 the dashed lines show the curves we supplied earlier based on regression analysis of strong-motion data by Abrahamson and Silva (written communication, 1995). The dashed lines indicate less nonlinearity than the solid lines. This is not surprising in view of the fact that the soils in Imperial Valley have relatively low rigidity compared with the average for the data set used by Abrahamson and Silva.

ACKNOWLEDGMENTS

This work was partially supported by the U.S. Nuclear Regulatory Commission.

REFERENCES

Anderson, J. G. and S. E. Hough (1984). A model for the shape of the Fourier amplitude spectrum of acceleration at high frequency, *Bull. Seism. Soc. Am.* **74**, 1969–1993.

Boore, D. M. (1996). SMSIM — Fortran programs for simulating ground motions from earthquakes: Version 1.0, *U.S. Geol. Surv. Open-File Rept.*, in preparation.

EPRI (1993). Guidelines for determining design basis ground motions, TR-102293, Electric Power Research Institute, 5 vol.

Hanks, T. C. and R. K. McGuire (1981). The character of high-frequency strong ground motion, *Bull. Seism. Soc. Am.* **71**, 2071–2095.

Hardin, B. O. and V. P. Drnevich (1972). Shear modulus and damping in soils: Design equations and curves, *Proc. Am. Soc. Civil Eng., J. Soil Mech. Found. Div.* **98**, 667–692.

Idriss, I. M. and H. B. Seed (1968). Seismic response of horizontal soil layers, *Proc. Am. Soc. Civil Eng., J. Soil Mech. Found. Div.* **94**, 1003–1031.

Idriss, I. M. (1990). Response of soft soil sites during earthquakes, Proceedings, Memorial Symposium to honor Professor Harry Bolton Seed, Berkeley, California, **2**, May, 1990.

Idriss, I. M. and J. I. Sun (1992). User's manual for SHAKE91: A computer program for conducting equivalent linear seismic response analyses of horizontally layered soil deposits, Center for Geotechnical Modeling, Department of Civil Engineering, University of California, Davis, California.

Joyner, W. B. and A. T. F. Chen (1975). Calculation of nonlinear ground response in earthquakes, *Bull. Seism. Soc. Am.* **65**, 1315–1336.

Ladd, C. C. and L. Edgers (1972). Consolidated-undrained direct-simple shear tests on saturated clays, *Research Report R72-82*, Department of Civil Engineering, Massachusetts Institute of Technology, Cambridge, Massachusetts.

Lee, M. K. W. and W. D. L. Finn (1982). Dynamic effective stress analysis of soil deposits with energy transmitting boundary including assessment of liquefaction potential, Soil Mechanics Series No. 38, Dept. Civil Eng., Univ. of British Columbia, Vancouver, Canada.

Pyke, R. (1979). Nonlinear soil models for irregular cyclic loadings,*Proc. Am. Soc. Civil Eng., J. Geotech. Eng. Div.* **105**, 715–726.

Schnabel, P., H. B. Seed, and J. Lysmer (1972). Modification of seismograph records

for effects of local soil conditions, *Bull. Seism. Soc. Am.* **62**, 1649–1664.

Seekins, L. C., A. G. Brady, C. Carpenter, and N. Brown (1992). Digitized strong-motion accelerograms of North and Central American earthquakes 1933–1986 (CD-ROM), U.S. Geol. Surv. Digital Data Series DDS-7.

Sun, J. I., R. Golesorkhi, and H. B. Seed (1988). Dynamic moduli and damping ratios for cohesive soils, Report No. UCB/EERC-88/15, Earthquake Engineering Research Center, University of California, Berkeley, California, 42 p.

Table 1. List of events used to study κ in the Imperial Valley

Date	Hr:Min	Magnitude	Lat.	Long.
20-Jun-75	05:48 A	4.2	32.780	115.433
04-Nov-76	05:48 B	3.9	33.143	115.538
20-Oct-77	10:29	4.0	32.886	115.498
21-Oct-77	13:24	4.0	32.898	115.507
30-Oct-77	05:30	4.0	32.893	115.505
14-Nov-77	00:11	3.7	32.832	115.480
14-Nov-77	02:05	4.1	32.830	115.478
14-Nov-77	05:36	4.0	32.835	115.481
14-Nov-77	12:20	4.2	32.822	115.467
11-Mar-78	05:40	3.6	32.316	115.106
11-Mar-78	23:57	4.9	32.308	115.108
12-Mar-78	00:30	4.5	32.345	115.129
12-Mar-78	18:42	4.8	32.307	115.110
16-Mar-78	01:51	4.1	32.327	115.113
10-Oct-79	19:48	4.0	32.382	115.330
15-Oct-79	23:16	6.5	32.658	115.330
15-Oct-79	23:19	5.1	32.773	115.427
16-Oct-79	06:58	5.5	32.999	115.569
21-Dec-79	20:40	4.8	32.484	115.194
21-Dec-79	20:58	3.5	32.381	115.167
09-Jun-80	03:28	6.1	32.185	115.076
09-Jun-80	10:00	4.5	32.297	115.134
09-Jun-80	23:33	4.3	32.365	115.215
26-Apr-81	12:09	5.6	33.098	115.618

Event	BRA	CAL	CX	CPR	CU	DLTA	E01	E02	E03	E04	E05	E06	E07	E08	E10	E11	EDA	HVP	NIL	PTS	SUP	VCT	WS
2316	X	X	X	X	X	X	X	X	X	X	X	X	X	X	X	X	X	X	X	X	X	X	X
2319	X		X			X	X	X	X	X	X	X	X	X	X	X	X	X					
A548												X											
B548		X																					
1029											X												
1324											X												
530											X			X									
11												X											
205												X		X									
536														X									
1220										X	X			X									
540																						X	
2357						X																X	
30																						X	
1842																						X	
151																						X	
1948				X																			
658																							X
2040																							
2058					X																		
328				X	X																		
1000				X																			
2333						X																	
1209	X																		X	X	X		X

Table 2. Event–station matrix. X indicates a recording used in the analysis.

Table 3. Regression results; "S10", etc, designate specific sites.

Regression Output:	
Constant	0.0000
Std Err of Y Est	0.0066
R Squared	0.8222
No. of Observations	69
Degrees of Freedom	41

AvgSite: 0.0309

	s10	s20	s30	s40	s50	s60	s70	s80	s90	s100	s110		
X Coefficient(s)	0.0235	0.0349	0.0316	0.0235	0.0224	0.0282	0.0157	0.0393	0.0441	0.0204	0.0298		
Std Err of Coef.	0.0064	0.0071	0.0060	0.0059	0.0066	0.0064	0.0072	0.0070	0.0070	0.0066	0.0053		
	s120	s130	s140	s150	s160	s170	s180	s190	s200	s210	s220	s230	MS=1
X Coefficient(s)	0.0260	0.0379	0.0293	0.0231	0.0478	0.0481	0.0413	0.0321	0.0382	0.0311	0.0167	0.0264	0.0060
Std Err of Coef.	0.0060	0.0074	0.0051	0.0070	0.0070	0.0071	0.0070	0.0075	0.0069	0.0075	0.0056	0.0064	0.0029

n= 1.000

	Dist	log(nV)	log(nV)^2	log(nV)^3
X Coefficient(s)	0.00026	-0.00122	0.02417	-0.01178
Std Err of Coef.	0.00012	0.02022	0.02361	0.00785

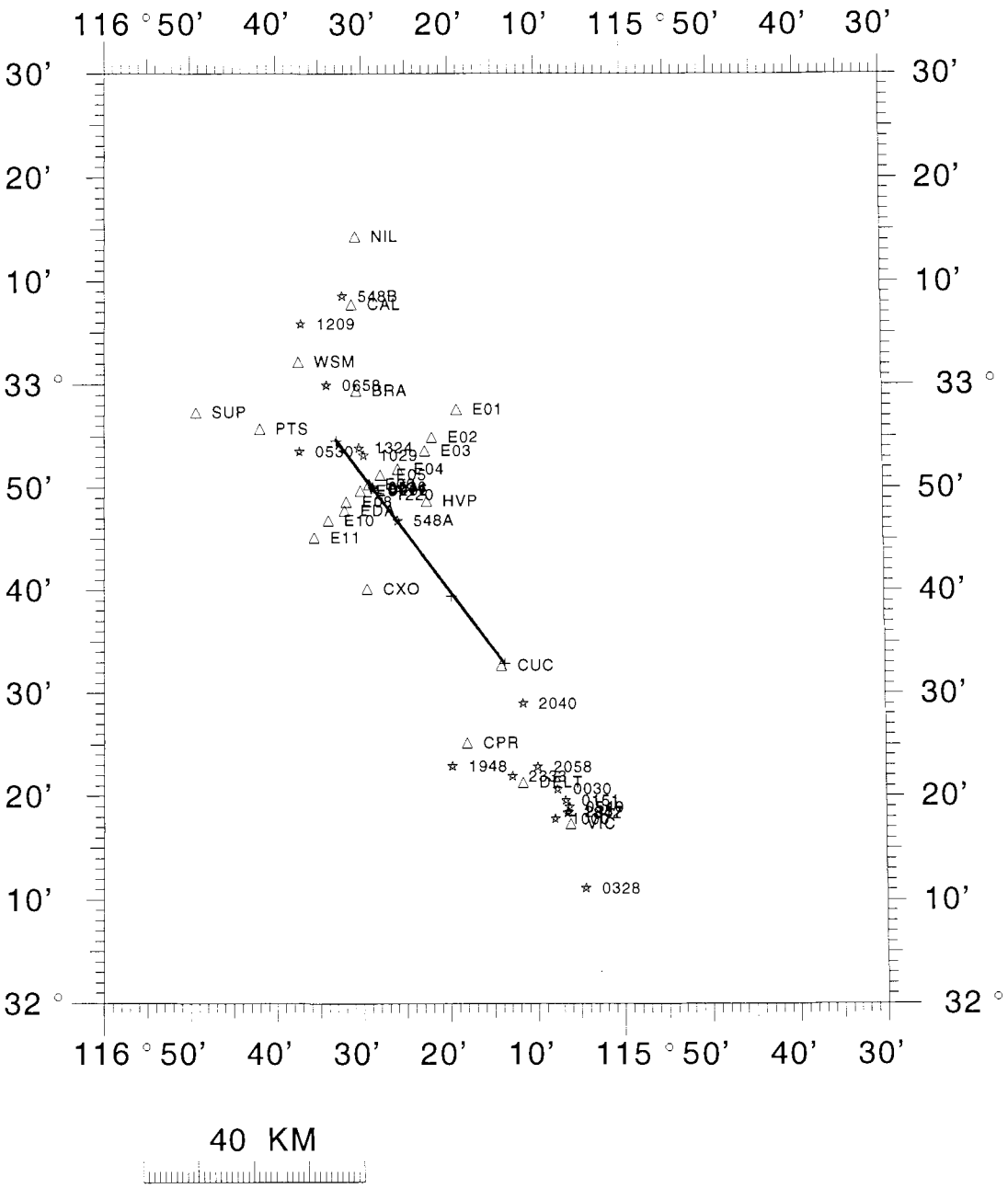

Figure 1. Map of Imperial Valley region showing stations (triangles) and events (mainshock = line; smaller events = stars) used in the analysis of κ.

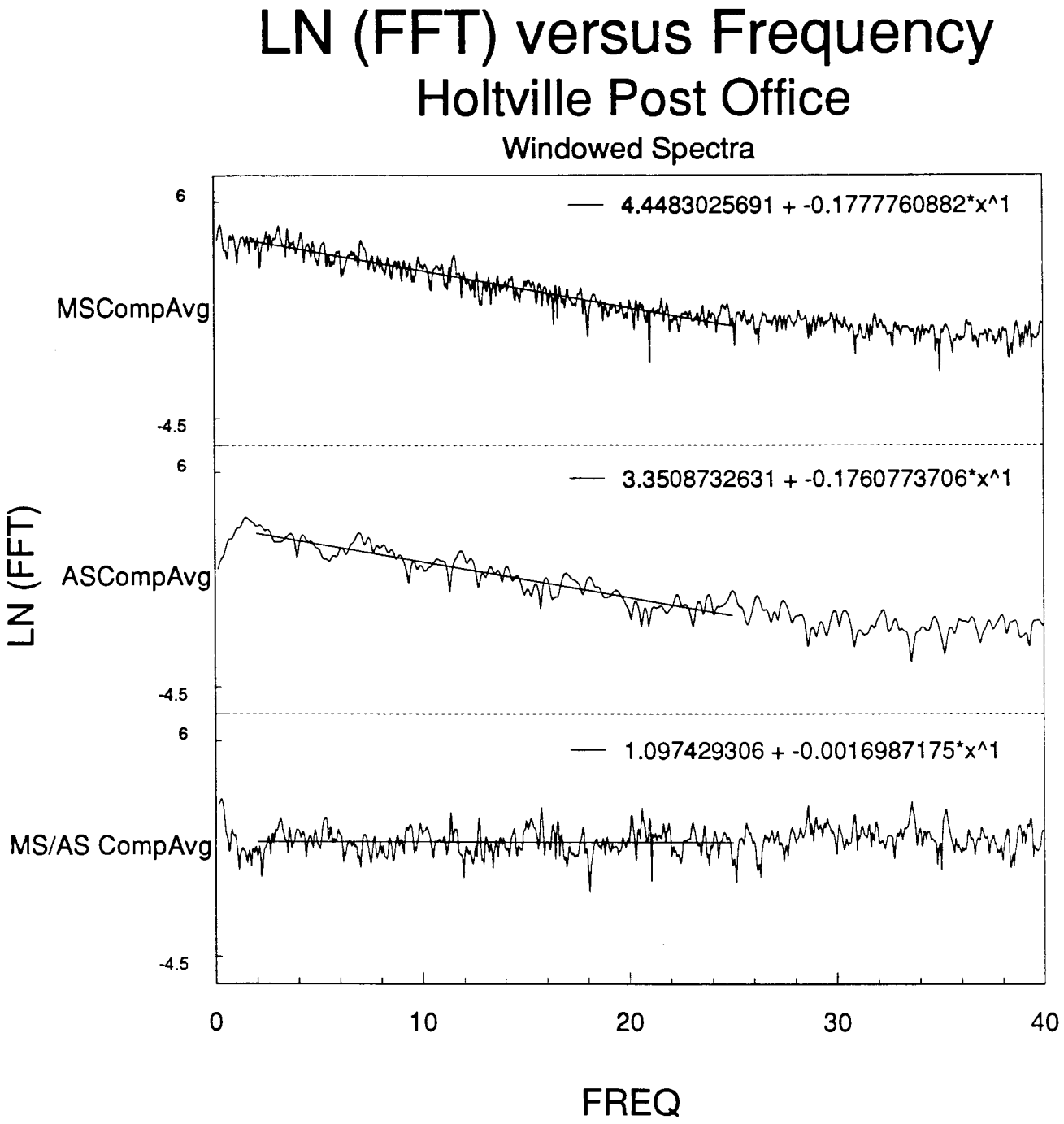

Figure 2. Example of spectra plotted on log–linear axes and fit of straight line to the spectra; κ is equal to the slope of the line divided by π. The top and middle panels are for the mainshock and 2319 aftershock recorded at Holtville; the bottom panel should be ignored.

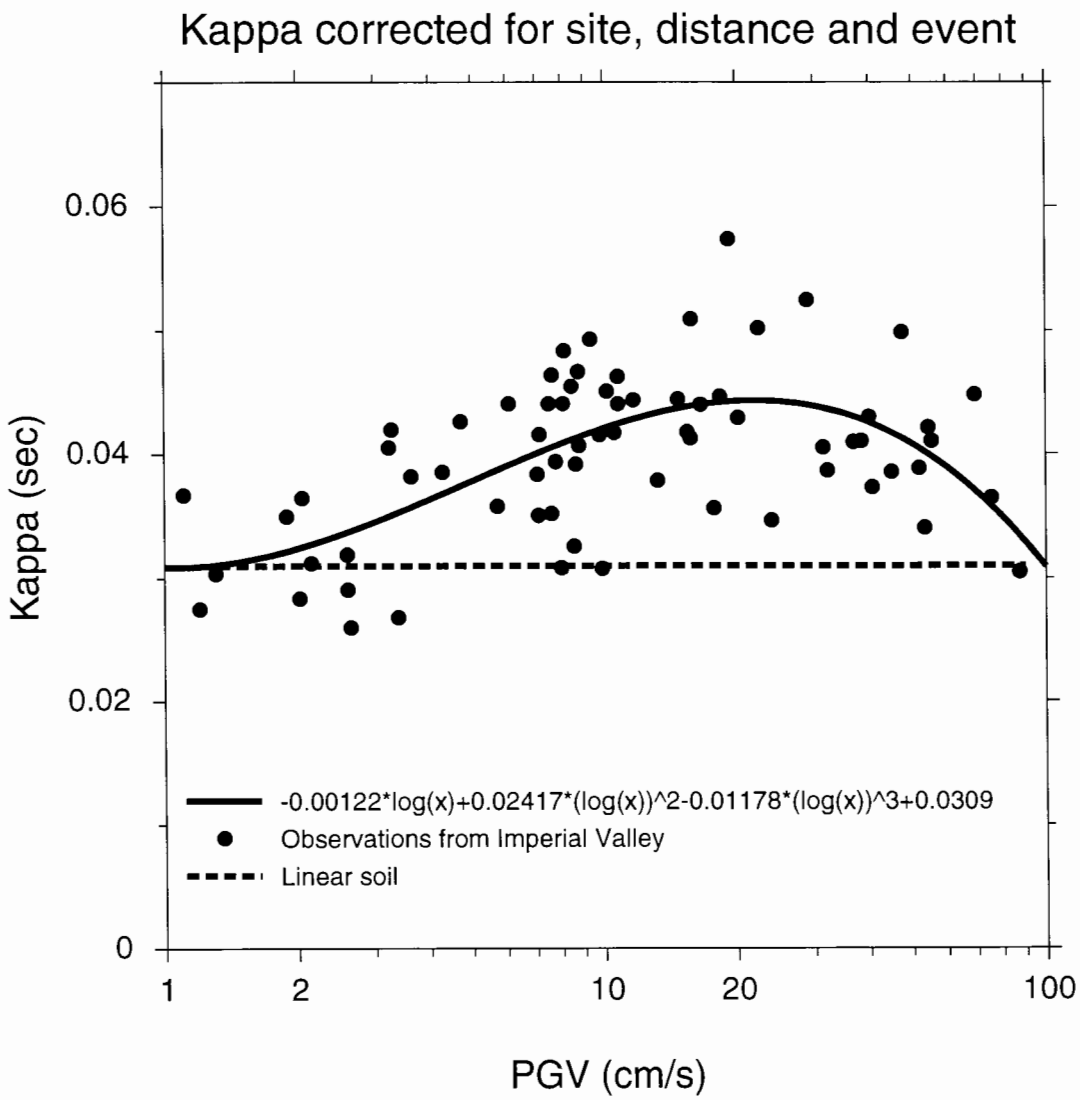

Figure 3. κ, corrected for distance, site, and event type (mainshock or not), plotted against peak velocity. The solid line is a least-squares fit using the functional form shown in the legend; the dashed line shows the relation if the soil response were perfectly linear.

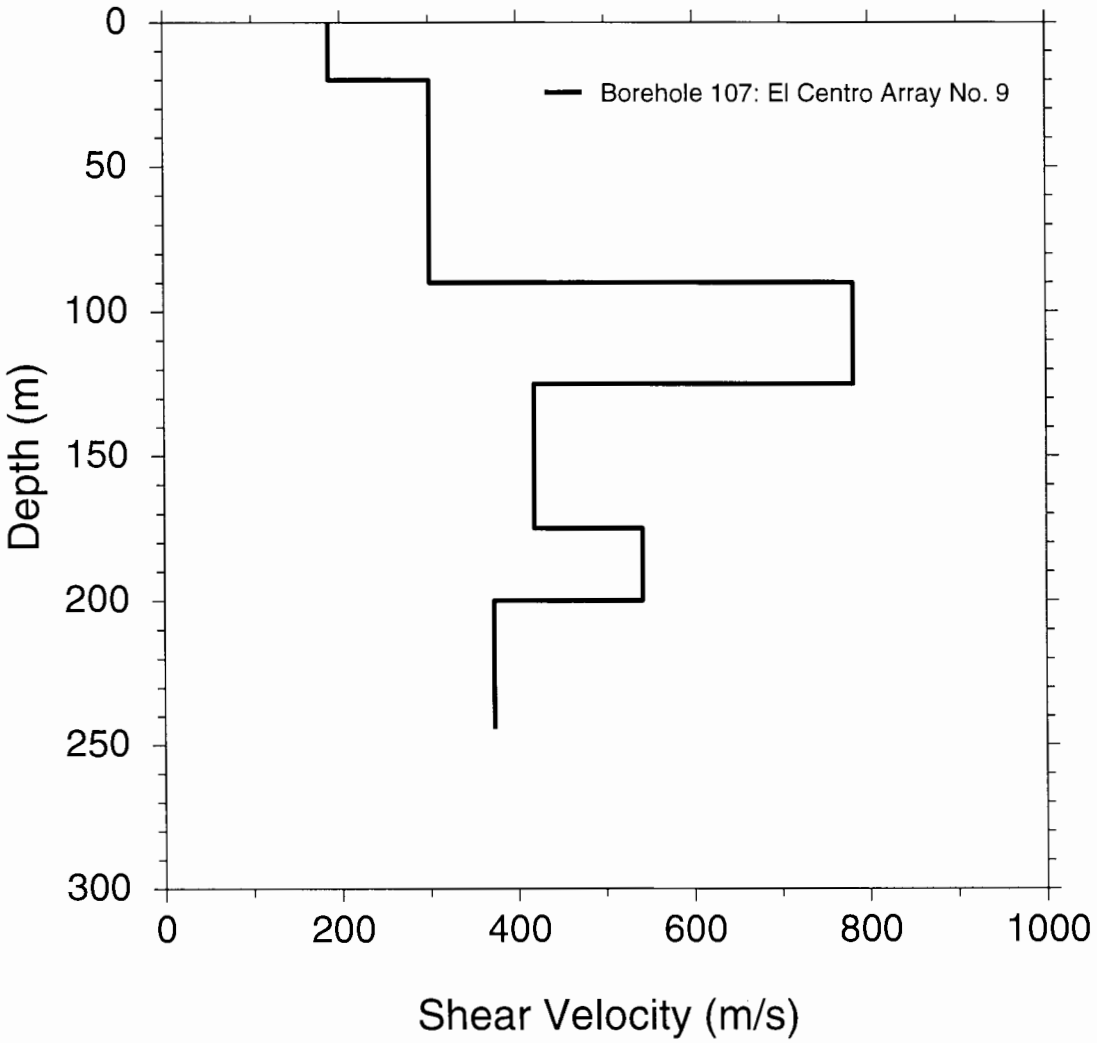

Figure 4. Shear-velocity as a function of depth from a borehole near the center of the Imperial Valley (the velocities were derived by fitting S travel times published by Porcella, 1984, with a piecewise-continuous series of straight lines).

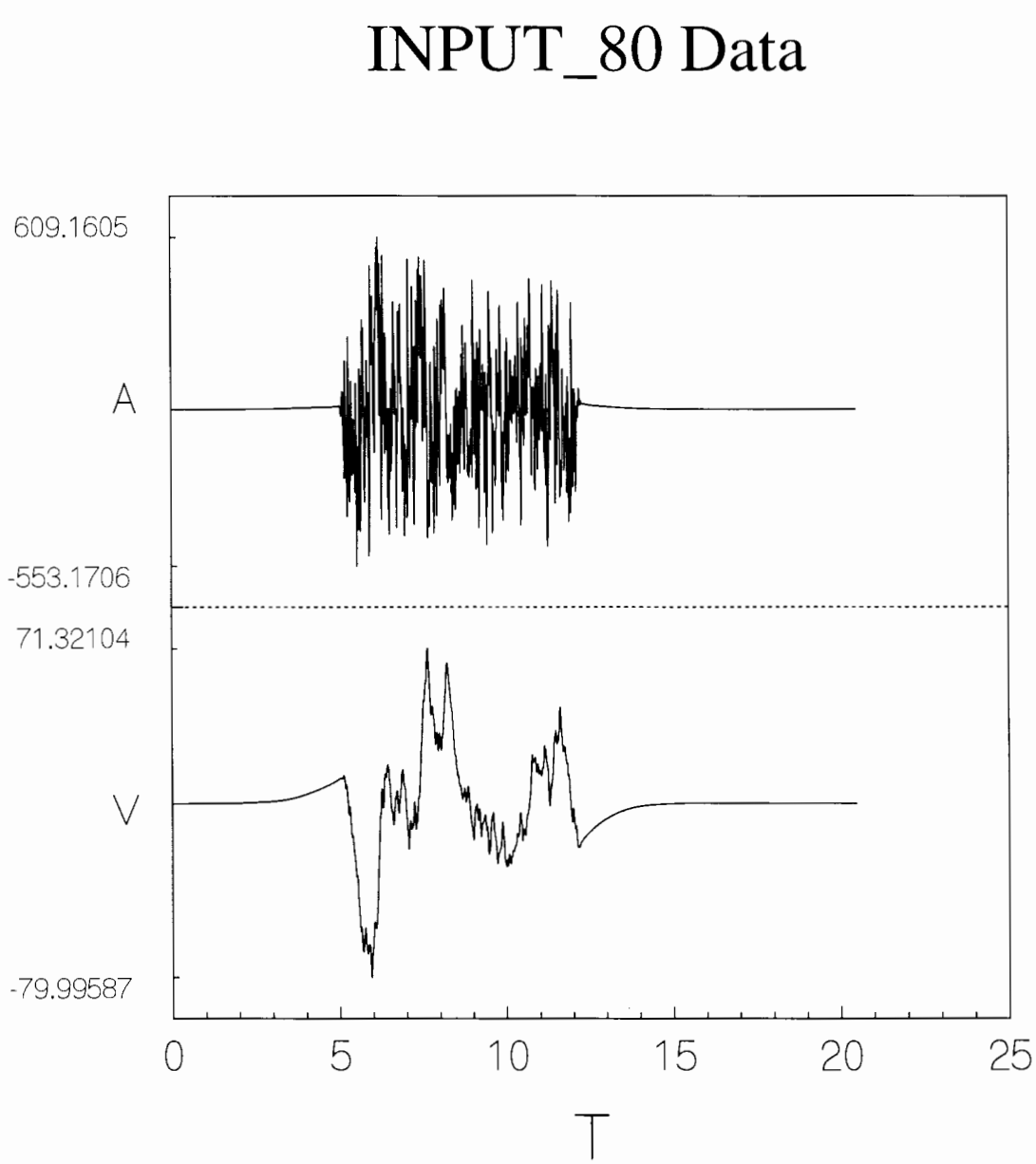

Figure 5. Acceleration and velocity time series used as input to the soil column in the nonlinear response analysis. The peak velocity is twice the amplitude of the waves *incident* on the base of the soil column (i.e., the peak velocity is the same as would be recorded at the surface of a uniform halfspace). The peak velocity here is 80 cm/s, but simulations were made using a range of peak velocities. The acceleration time series was derived from the stochastic model of Boore (1996), using a rock amplification, source velocity of 3.3 km/s, and a stress parameter of 70 bars.

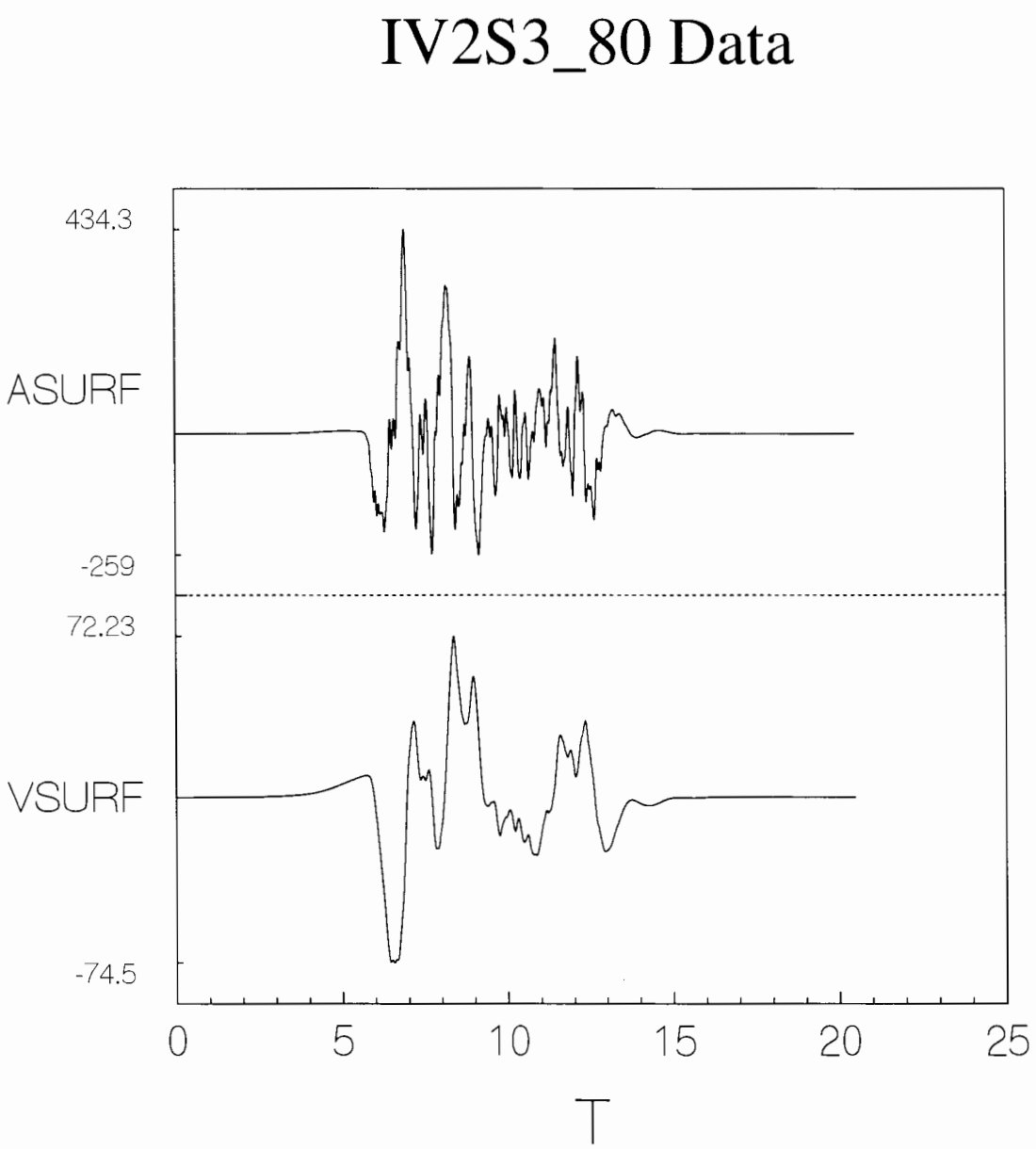

Figure 6. Acceleration and velocity time series at the surface of the 90 m–thick soil column from SHAKE91, using an input motion whose equivalent peak velocity at the surface of a uniform halfspace would be 80 cm/s.

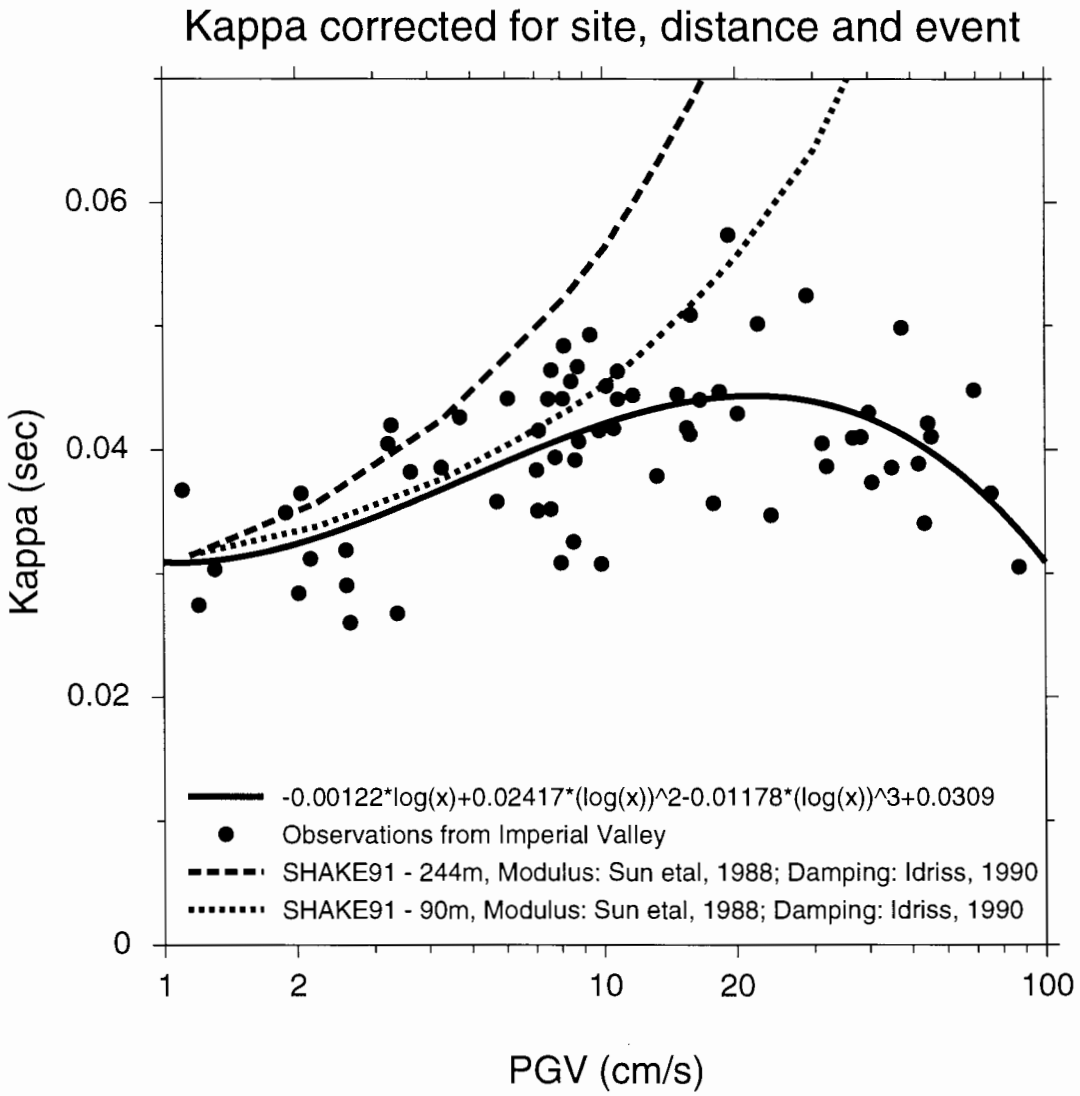

Figure 7. Comparison of κ's derived from SHAKE91 and the data.

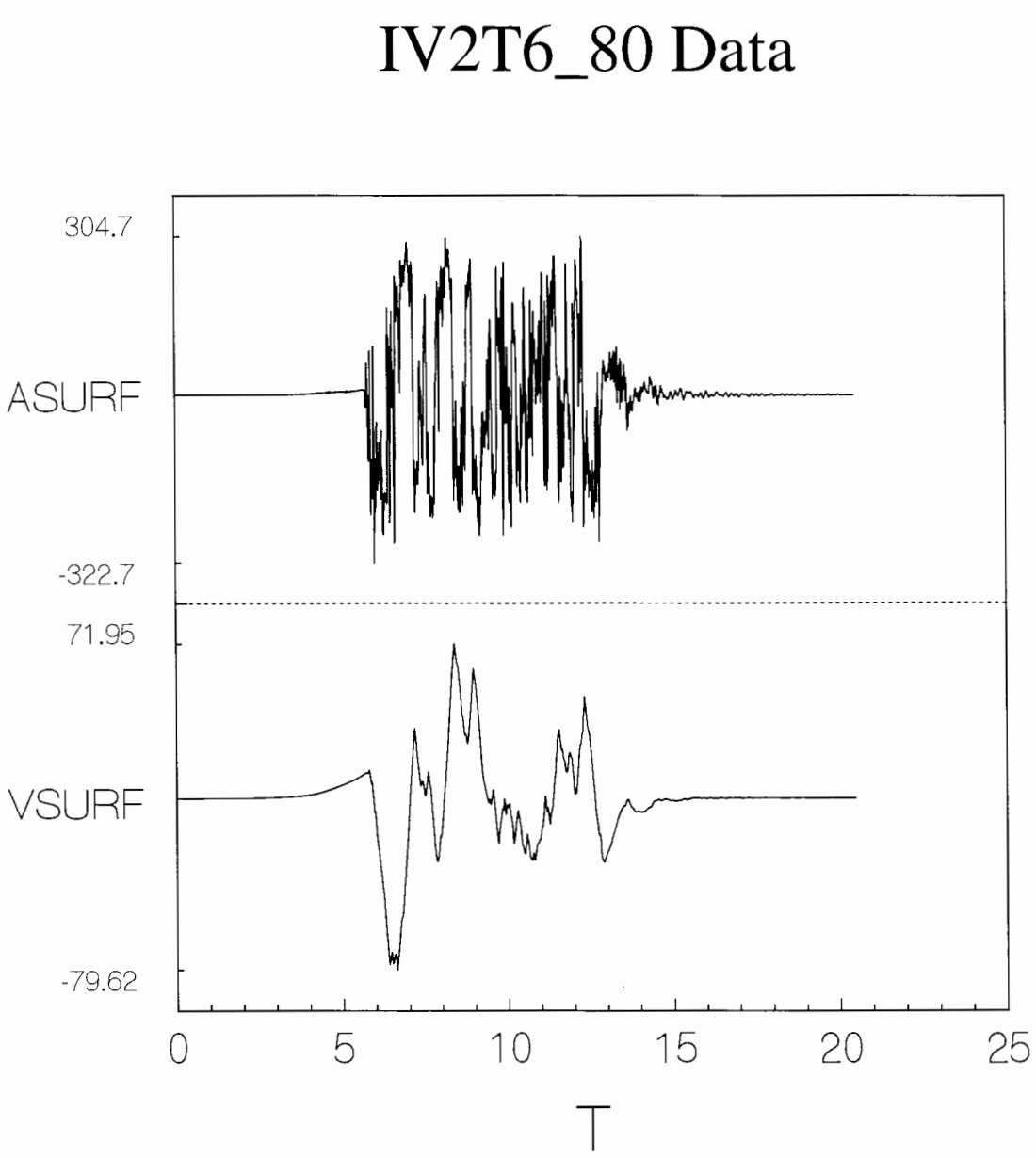

Figure 8. Acceleration and velocity time series at the surface of the 244 m–thick soil column from TESS, using an input motion whose equivalent peak velocity at the surface of a uniform halfspace would be 80 cm/s.

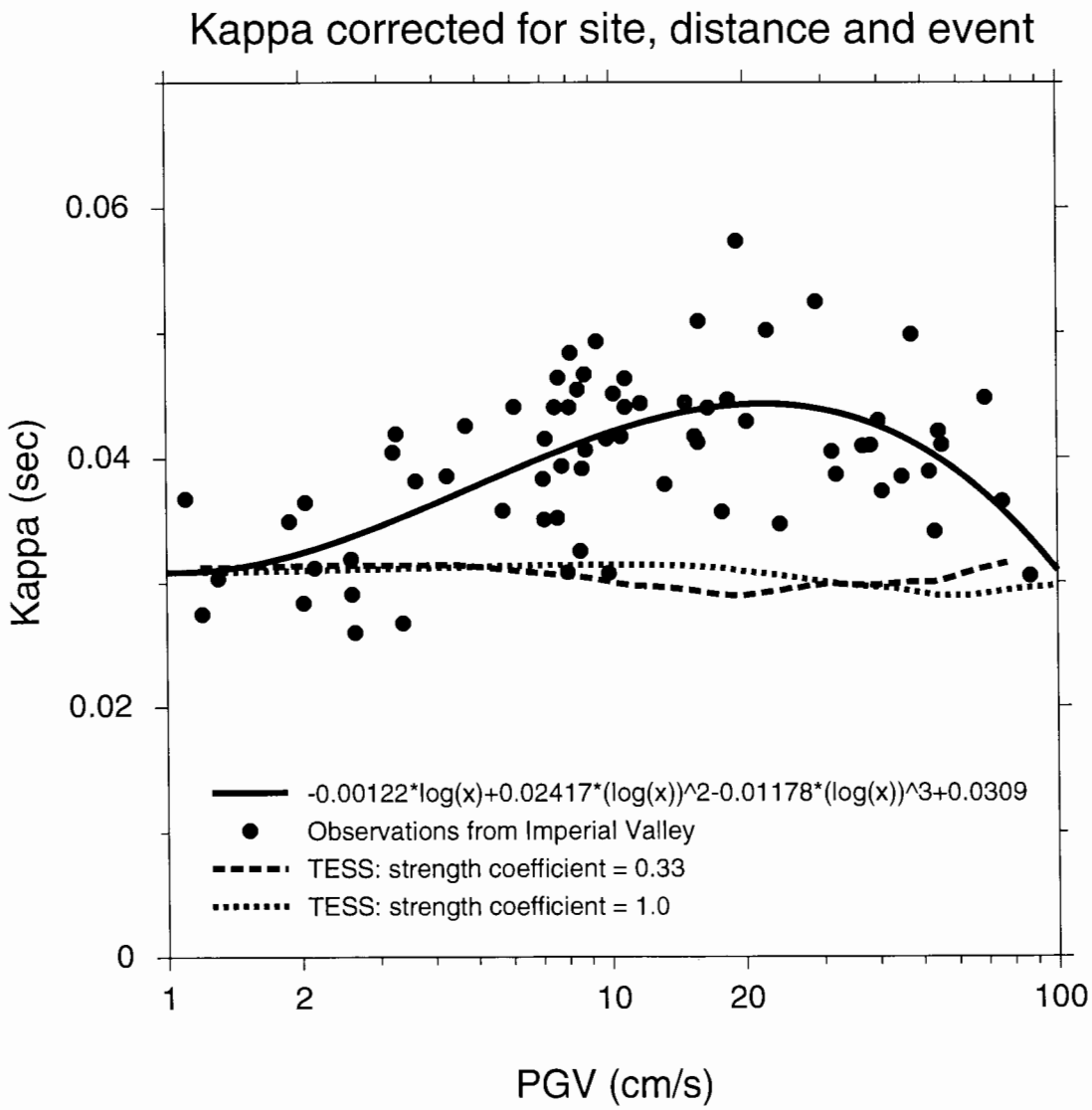

Figure 9. Comparison of κ's derived from TESS, using two values for the strength coefficient, and the data.

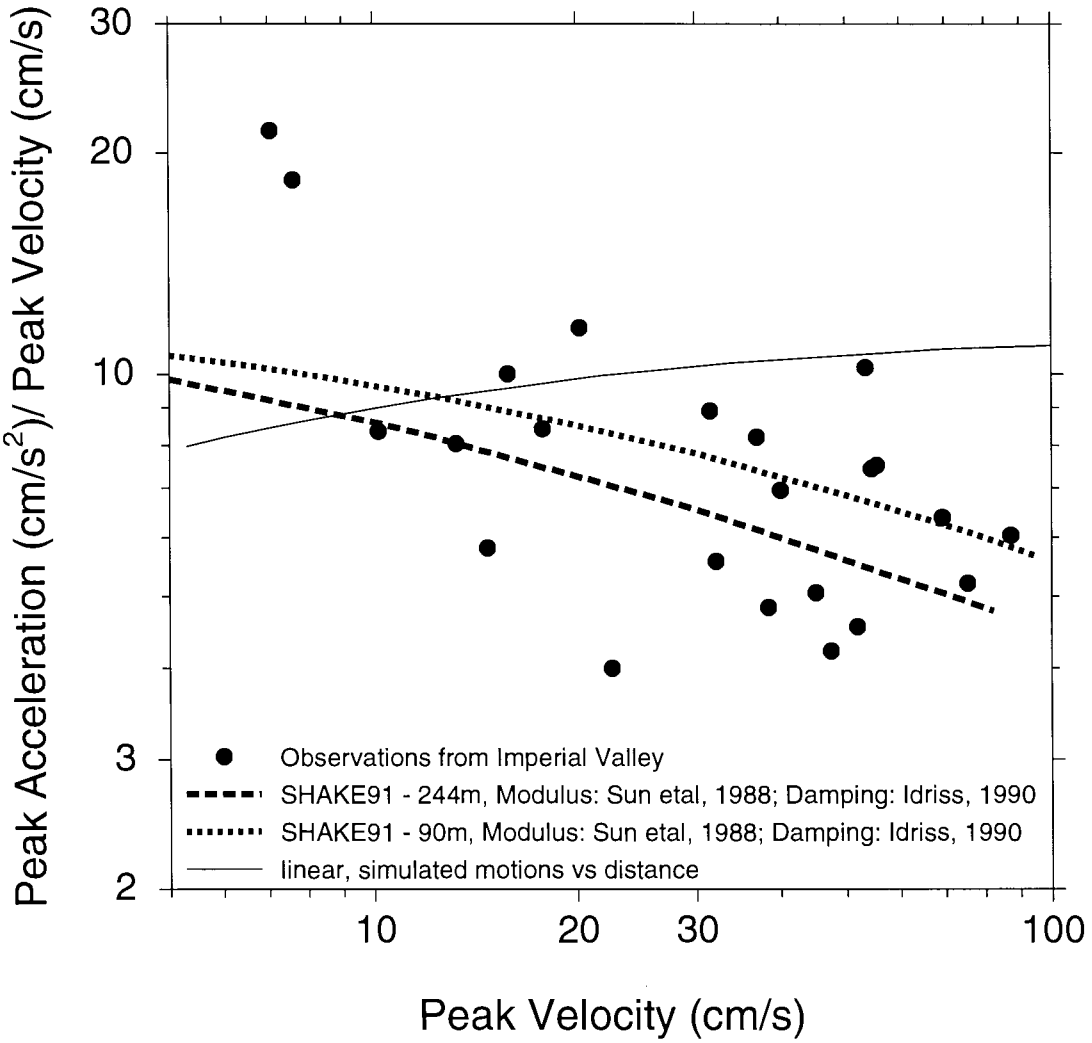

Figure 10. Ratio of peak acceleration to peak velocity, as a function of peak velocity. The data are given by filled circles, the results of simulations using the stochastic model by the light line, and the results from SHAKE91 by the dashed lines. SHAKE91 was used with two soil columns: 244m thick and 90m thick (the upper 90m being the same in both models). The observed values are the geometric mean of the two horizontal components.

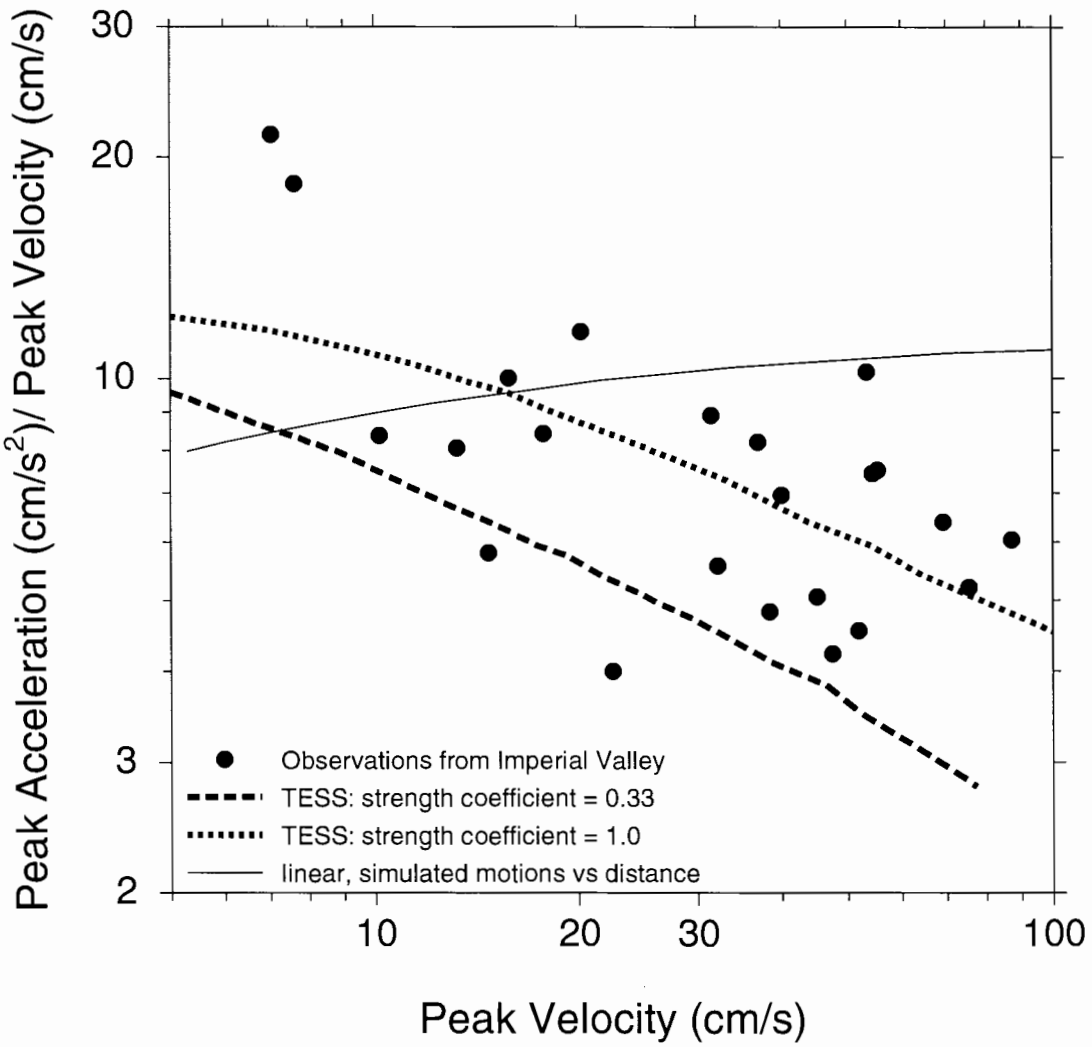

Figure 11. Ratio of peak acceleration to peak velocity, as a function of peak velocity. The data are given by filled circles, the results of simulations using the stochastic model by the light line, and the results from TESS by the dashed lines. Two values of the strength coefficient were used in TESS. The observed values are the geometric mean of the two horizontal components.

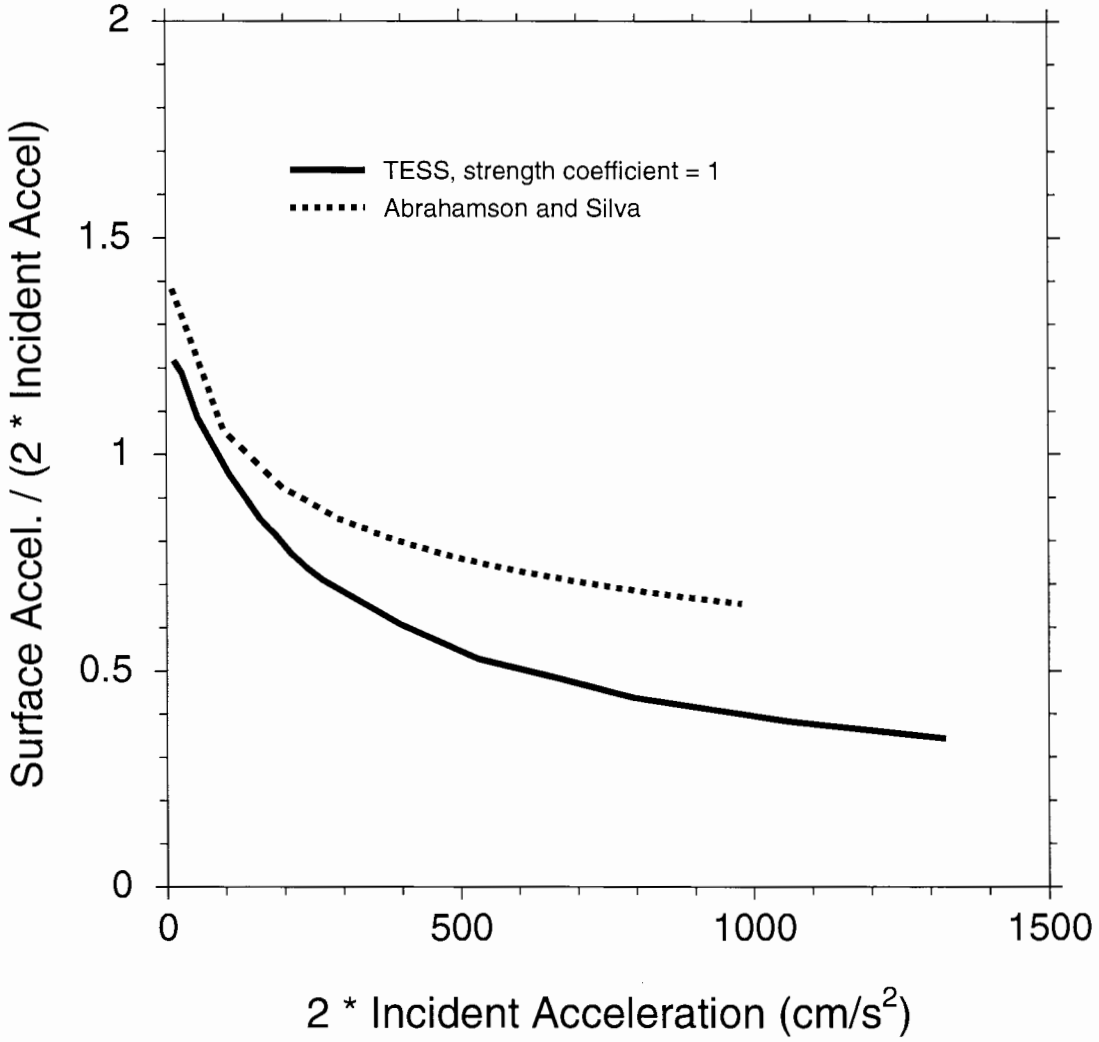

Figure 12. The figure is an approximation of the ratio of the peak acceleration at the surface of the soil column to the peak acceleration at the base, as a function of the peak motion at the base. The solid line comes from calculations using TESS with a strength coefficient of 1.0, and the dashed curve is from the empirical attenuation relations of Abrahamson and Silva (1996), with their soil motions divided by their rock motions.

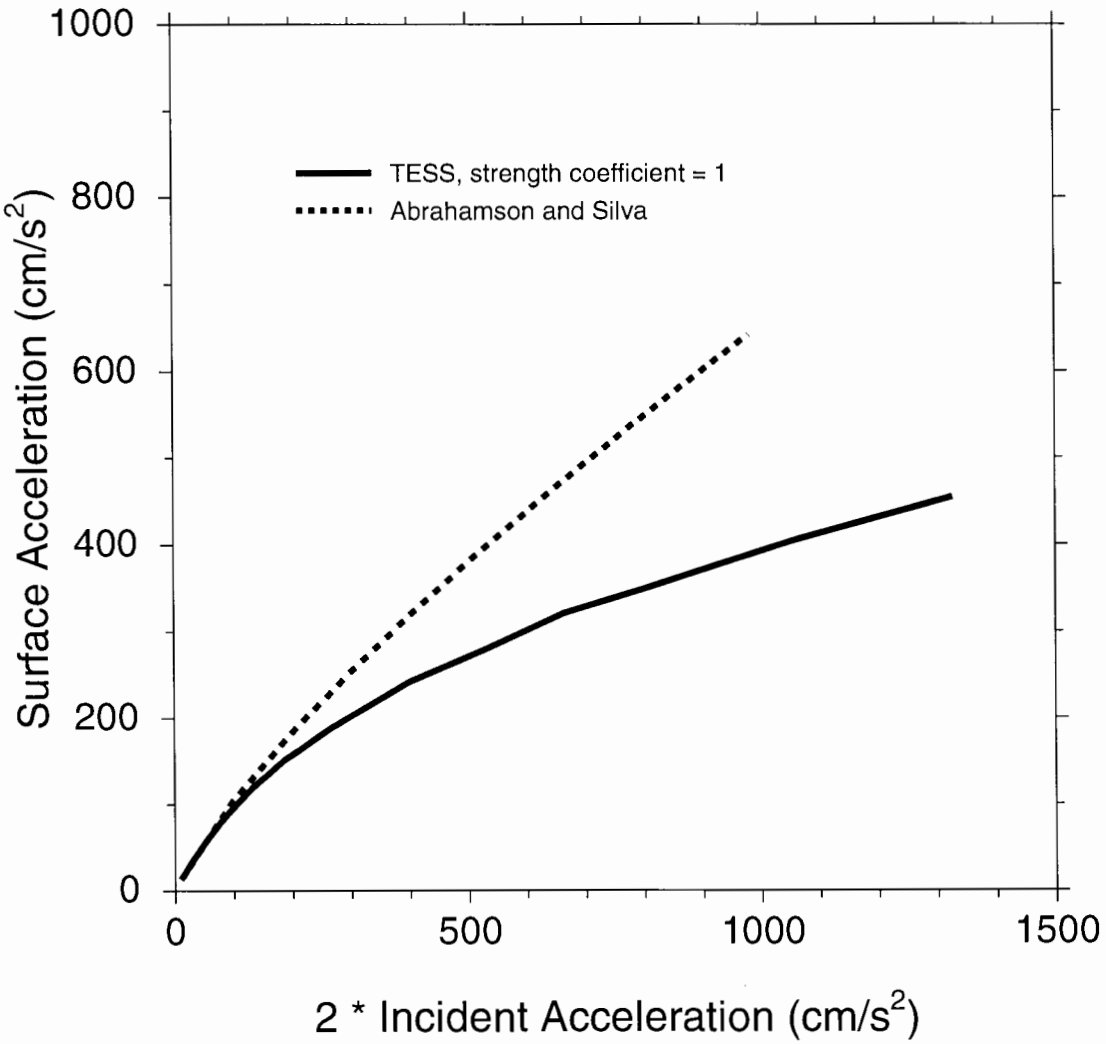

Figure 13. The figure is an approximation of the peak acceleration at the surface of the soil column as a function of the peak motion at the base. The solid line comes from calculations using TESS with a strength coefficient of 1.0, and the dashed curve is from the empirical attenuation relations of Abrahamson and Silva (1996), with their soil motions divided by their rock motions.